Journal of Radiation Research, Vol. 62, No. 5, 2021, pp. 793–803
https://doi.org/10.1093/jrr/rrab045
Advance Access Publication: 1 June 2021

Assessment of cellular and molecular changes in the rat brain after gamma radiation and radioprotection by anisomycin

Dušica M. Kočović[1], Danica Bajuk-Bogdanović[2], Ilinka Pećinar[3], Biljana Božić Nedeljković[4], Marko Daković[2] and Pavle R. Andjus[1,*]

[1]Center for Laser Microscopy, Faculty of Biology, University of Belgrade, Studentski Trg 3, 11 000 Belgrade, Serbia
[2]Faculty of Physical Chemistry, University of Belgrade, Studentski Trg 12-16, 11 000 Belgrade, Serbia
[3]Faculty of Agriculture, Department for Agrobotany, University of Belgrade, Nemanjina 6, 11 080 Belgrade, Serbia
[4]Institute for Physiology and Biochemistry "Jean Giaja", Faculty of Biology, University of Belgrade, Studentski Trg 3, 11 000 Belgrade, Serbia
*Corresponding author. Pavle R. Andjus, Center for Laser Microscopy, Faculty of Biology, University of Belgrade, Studentski Trg 3, 11 000 Belgrade, Serbia.
Tel: +381-11-3032356; Fax: +381-11-2638-500; E-mail: pandjus@bio.bg.ac.rs
(Received 12 March 2021; revised 31 March 2021; editorial decision 26 April 2021)

ABSTRACT

The objective of the study was to describe cellular and molecular markers of radioprotection by anisomycin, focusing on the changes in rat brain tissue. Two-month-old Wistar rats were exposed to a ^{60}Co radiation source at a dose of 6 Gy, with or without radioprotection with anisomycin (150 mg/kg) administered subcutaneously 30 min before or 3 or 6 h after irradiation. Survivors were analyzed 30 days after treatment. Astroglial and microglial responses were investigated based on the expression of glial markers assessed with immunohistochemistry, and quantitative changes in brain biomolecules were investigated by Raman microspectroscopy. In addition, blood plasma levels of pro-inflammatory (interleukin 6 and tumor necrosis factor α) and anti-inflammatory (interleukin 10) cytokines were assessed. We found that application of anisomycin either before or after irradiation significantly decreased the expression of the microglial marker Iba-1. We also found an increased intensity of Raman spectral bands related to nucleic acids, as well as an increased level of cytokines when anisomycin was applied after irradiation. This suggests that the radioprotective effects of anisomycin are by decreasing Iba-1 expression and stabilizing genetic material by increasing the level of nucleic acids.

Keywords: gamma radiation; radioprotectors; anisomycin; Raman microspectroscopy; glial cells; cytokines

INTRODUCTION

The brain can be acutely affected by radiotherapy or accidental irradiation [1]. Radioprotectors are agents that have the potential to protect healthy tissue from the cytotoxic effects of gamma and X-rays during therapeutic or diagnostic procedures, but may also be applied after accidental radiation events. Although a large variety of natural and synthetic compounds have been tested, only amifostine (WR-2721) is currently in clinical use. However, its application has some side effects and limitations, particularly when used to protect central nervous tissue [2, 3].

The antibiotic anisomycin, a compound isolated from *Streptomyces griseolus* bacteria, is one of several novel potential radioprotectors [4]. The principal action of anisomycin is to inhibit protein synthesis at the translational step by binding to 60S ribosomal subunit, thus blocking peptide bond formation [5, 6]. It was found that anisomycin may affect stress-activated protein kinase cascades, the c-Jun N-terminal kinase (JNK) pathway, as well as the p38 mitogen-activated protein kinase (MAPK) pathways in mammalian cells, all of which are neuroprotective in the brain [7, 8]. In fact, it has been shown that anisomycin has a significant role in the protection of cortical neurons in culture from prolonged hypoxia, as well as of other cell types under stress [9–11]. Also noteworthy is the finding that the highest tissue concentration of anisomycin administered to rats is in the brain, further motivating the study of its use to protect against radiation-induced brain injury [12].

The aim of this study was to investigate the effects of anisomycin on irradiated rats by applying it before (as in the case of radiotherapy), or hours after irradiation (as in the case of accidental irradiation). The main goal was to characterize cellular and molecular signatures

of radioprotection in surviving animals. The area of interest was the brainstem, since this is one of the most radiosensitive parts of the brain [13]. We also assessed changes in the corpus callosum, the largest white matter tract in the brain, as well as in the somatosensory cortex, part of the outermost and thus most highly radio-exposed layer of the brain. It is known that radiation damage is prominent in the brainstem and corpus callosum [14].

Our immunohistochemical assessment revealed a significant decrease in Iba-1 expression, which we interpret as a decrease in microglial abundance, in all three investigated brain areas following radioprotection by anisomycin, indicating that anisomycin acts against radiation-induced neuroinflammation. Molecular fingerprinting by Raman microspectroscopy showed an increased intensity of bands related to nucleic acids in the irradiated brainstem in all groups treated with anisomycin, both before and after radiation, suggesting a stabilization of the genetic material. In addition, spectral bands related to amino acids were also increased with the application of anisomycin after irradiation. Anisomycin also increased plasma levels of pro-inflammatory and anti-inflammatory cytokines, with the effect being greater for application after irradiation and if checked at later time points. These results were consistent in all surviving animals (75% survival for pre-radiation application, 100% for post-radiation application). Overall, these results indicate that the radioprotective effect of anisomycin is mediated at least in part through modulating neuroinflammation and nucleic acid stability.

MATERIALS AND METHODS

Animals

Two-month-old male albino Wistar rats, weighing approximately 200 g, were housed in Vinca, Institute of Nuclear Science, under standard laboratory conditions (room temperature 21 ± 1°C, humidity 30%, and under 12/12 h light/dark cycle) with food and tap water ad libitum. All experiments were performed in accordance with the 3 Rs principle and the EU directives on the protection of animals for scientific purposes and with permission from the Ethical Commission of the Faculty of Biology, University of Belgrade (approval number EK-BF-2016/08).

Survival analysis

Survival in all five experimental groups was monitored throughout the experiment from the first day until the thirtieth day. Survival probabilities were plotted as Kaplan–Meier survival curves. Significant differences in the survival curves among experimental groups were evaluated using the log-rank (Mantel-Cox) test for multiple groups.

Irradiation protocol and treatment with anisomycin

A 6 Gy ($LD_{50/30}$) dose of gamma radiation from a ^{60}Co source was applied as whole-body irradiation. Non-anesthetized, immobilized animals were placed in separate cages arranged in a circle around the radiation source. The cages were rotated 180° at the midpoint of the irradiation session to ensure symmetrical radiation of the body. Anisomycin was administered subcutaneously in a single dose, 150 mg/kg body weight, which is the standard dose in pharmacological studies with this agent [15]. There were six experimental groups. The control group (CTRL) comprised non-treated naïve animals. The radioprotector control group (AN) received anisomycin in the absence of irradiation. The irradiated-only group (Irr) consisted of irradiated animals that did not receive anisomycin. To investigate the radioprotective potential of anisomycin as a function of time of administration, three additional experimental groups comprised respectively of rats receiving a single dose of anisomycin 30 min prior to irradiation (ANIr-30), 180 min after irradiation (ANIr180) and 360 min after irradiation (ANIr360). Each experimental group contained n = 4 rats, except the Irr group, in which we doubled the number of animals (n = 8) to compensate for an expected higher mortality rate (Fig. 1). During the 30 days after irradiation, blood plasma was collected for ELISA tests for the analysis of cytokines. After 30 days, surviving animals were anesthetized by i.p. injection of ketamine and xylazine (1 mL/kg body weight), transcardially perfused with 0.9% NaCl solution and 4% paraformaldehyde (PFA) in 0.1 M phosphate buffer. The rats were then decapitated by guillotine and the brains were removed. One cerebral hemisphere and one half of the brainstem of each animal was taken for immunohistochemistry, while the other hemisphere and half-brainstem was taken for Raman microspectroscopy.

Immunohistochemistry

One cerebral hemisphere and one half brainstem from each animal were fixed with 4% PFA in 0.1 M PB for 24 h at 4°C, after which the tissue was cryoprotected in 30% sucrose in 0.1 M PB and then cryoembedded. Sections (30 μm) were cut in the coronal plane with a cryostat (Leica Microsystems, Germany) and mounted on gelatin-coated glass coverslips. Sections were collected from two brain regions: 10.35 mm (brainstem) and 2.45 mm (contain somatosensory cortex and corpus callosum) from Bregma according to a rat brain atlas [16], and thus contained the gigantocellular reticular nucleus of the brainstem, the somatosensory cortex, and the corpus callosum. Sections were permeabilized and blocked with 10% bovine serum in phosphate buffered saline (PBS) containing 0.2% Triton X-100. Primary antibodies were diluted in 2% bovine serum blocking solution and applied overnight at 4°C with the following dilutions: polyclonal goat anti Ionized calcium binding adaptor molecule 1 (Iba-1), 1:250 (Abcam, USA) and polyclonal rabbit anti Glial Fibrillary Acidic Protein (GFAP); 1:500 (Dako, USA). The negative control for Iba-1 and GFAP was performed by omitting the primary antibodies. Sections were rinsed 5 × 10 min in PBS, and secondary antibodies (Alexa Fluor 488 donkey-anti goat and Alexa Fluor 555 donkey-anti rabbit, both from Invitrogen, USA) were applied for 2 h at room temperature. Sections were rinsed 5 × 10 min with PBS and stained with the nuclear stain ToPro (1:4000; Invitrogen, USA). After final washes with PBS, the sections were coverslipped with glycerol (Mowiol, Sigma-Aldrich, Germany). Image acquisition was done on a Zeiss LSM 510 confocal laser scanning microscope (objective lenses Plan-Apochromat 40X oil) with Argon (488 nm) and Helium-Neon (543 nm and 633 nm) lasers. Analysis of obtained images was performed using ImageJ software to calculate the percentage of pixels per image frame. We analyzed three animals from each group with two sections stained from each animal and four (corpus callosum and brainstem) or eight (somatosensory cortex) images taken from each section. Thus, we obtained 24 or 48 data points from each animal group, respectively.

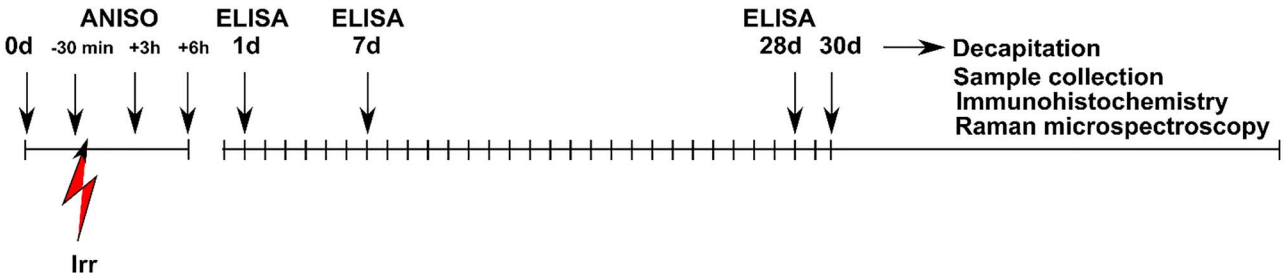

Fig. 1. Experimental timeline for studing the radioprotective potential of anisomycin. Gamma irradiation and anisomycin treatment were both performed on day 0. The exact time of each single anisomycin subcutaneous administration defined experimental groups (either –30 min before irradiation, +3 h, or +6 h after irradiation). Blood plasma for ELISA was taken on the first, seventh and 28th day after treatment. Decapitation and collection of samples for immunohistochemistry and Raman microspectroscopy were performed on day 30.

Tissue preparation for Raman spectroscopy; Raman instrumentation and analysis

The part of the brain for Raman spectroscopy was dissected out and stored at –80°C. Coronal sections were cut on a cryostat at 20 μm thickness and mounted on calcium fluoride microscope slides. Brain coordinates for sample collection were the same as for immunohistochemistry but from the opposite hemisphere. Raman spectroscopy was performed with an XploRA Raman spectrometer (Horiba Jobin Yvon) on sections of brainstem, somatosensory cortex and corpus callosum of all experimental groups. Raman scattering was excited by a frequency-doubled Nd/YAG laser at a wavelength of 785 nm (maximum output power 125 mW) equipped with 1800 lines/mm grating. Spectra were accumulated from 20 scans, with 60 s per scan. The spectral resolution was 2 cm^{-1} and calibration was checked for the 520.47 cm^{-1} line of silicon. The spectral range analyzed was in the interval from 600 to 1800 cm^{-1}. Removal of spike artefacts caused by cosmic rays was performed with the spectroscopic software Spectragryph, ver 1.2, and Raman processing with normalization of the spectra to the maximum signal intensity was performed in Matlab software package, version 2010a (The MathWorks, Natick, Massachusetts, USA). Further processing of the results involved the creation of differential spectra between the CTRL and Irr groups, and between the Irr and each radioprotected group (ANIr-30, ANIr180 and ANIr360), as well as assignation of spectral bands. Normalized signal intensities were used for statistical analysis. Three animals were analyzed from each group; four spectral scans were taken for one mean spectrum per section.

Detection of plasma cytokines by ELISA

Blood for plasma was extracted from the tail vein on the first, seventh and 28th days after treatment (Fig. 1). Blood plasma was stored at –70°C until assay. The concentration of cytokines (TNF-α, IL-6, IL-10) was measured according to the manufacturer's instructions for the ELISA assay (R&D Systems, Minneapolis, USA). The cytokine level was calculated using a reference curve constructed using known amounts of recombinant cytokines.

Statistical analysis

Data were analyzed using two-way ANOVA with the Bonferroni post hoc test. If the data were not normally distributed or the homogeneity of variance between groups was not met, the data were power transformed and then analyzed using the appropriate test. Immunohistochemical data were analyzed using ANOVA with repeated measures, followed by Dunnett's post hoc test, and cytokine data were analyzed using one-way ANOVA with the Holm-Sidak post hoc test. Statistical analyses were performed with the IBM SPSS Statistics 20 software package. Data are presented as mean ± SEM. Differences were considered significant with $P < 0.05$.

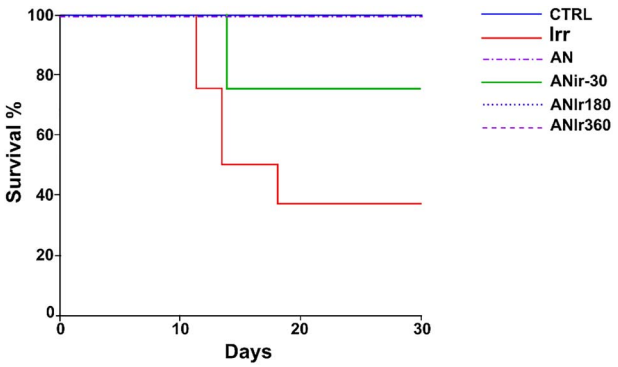

Fig. 2. Survival of rats in different experimental groups. Comparison of percentage of surviving rats among the six groups CTRL, Irr, AN, ANIr-30, ANIr180 and ANIr360, using Kaplan–Meier survival analysis. The survival curves for the CTRL and AN group, as well as for the ANIr180 and ANIr360 were significantly different in comparison with the Irr group as estimated by log-rank test ($P < 0.05$). The survival curve for the ANIr-30 group was not significantly different when compared to the Irr group.

RESULTS

Survival analysis

To verify the general radioprotective potential of anisomycin, we first followed the survival of animals with anisomycin administered at different time points before or after irradiation. Only 37.5% of animals (n = 3/8) survived the applied dose of gamma radiation in the absence of anisomycin treatment (Irr group). The survival of animals treated

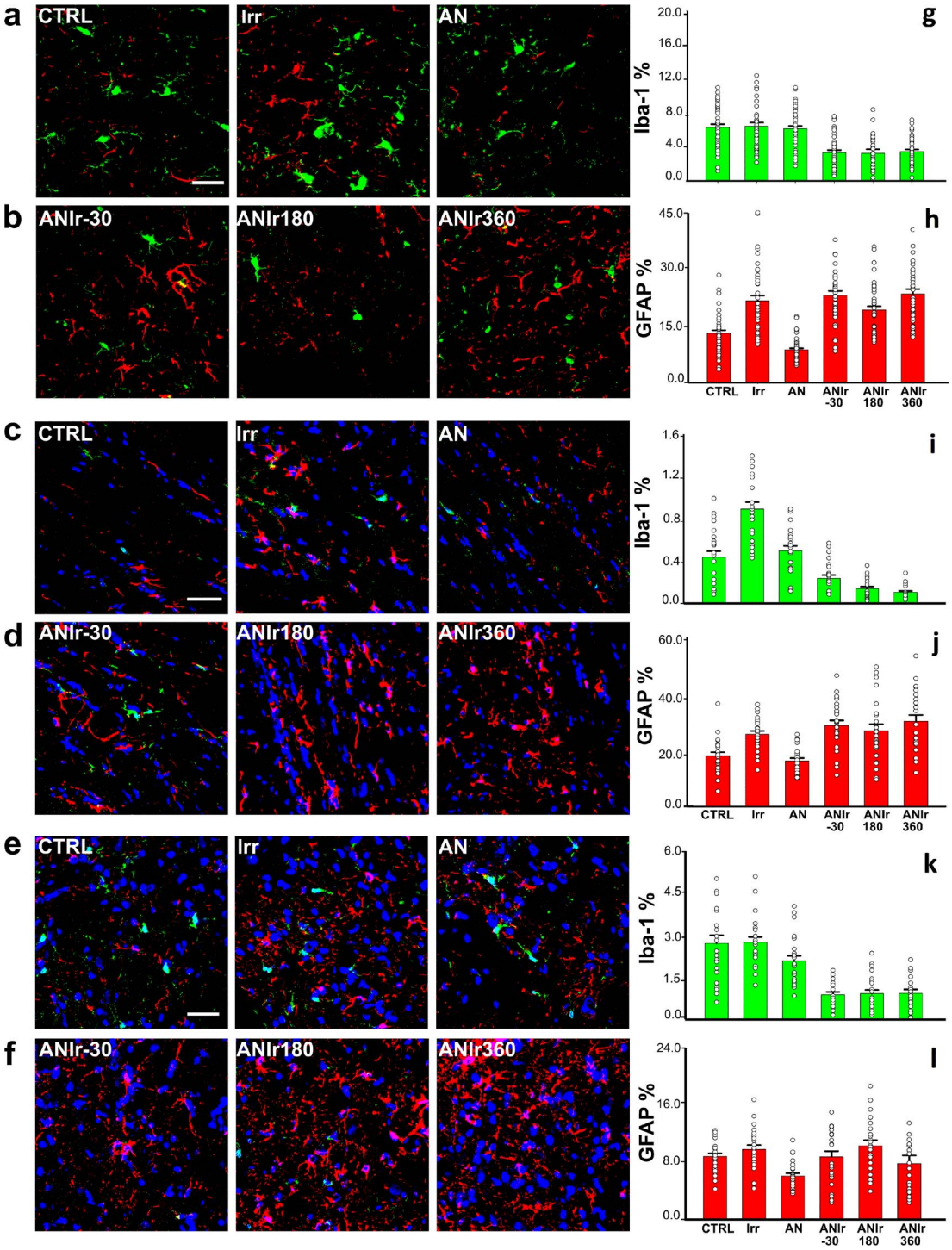

Fig. 3. Microglial and astroglial responses to gamma radiation, anisomycin administered alone, before or after irradiation detected in different brain structures: rat somatosensory cortex—panel rows (a, b); corpus callosum—panel rows (c, d); and brainstem—panel rows (e, f). Representative confocal images of immunofluorescence staining for Iba-1 (green) as a marker of microglial cells and GFAP (red) as a marker of astrocytes; in panel rows (c–f) nuclei are stained with ToPro (blue). CTRL—untreated naïve animals; Irr—whole body irradiated animals; AN—animals treated with anisomycin only; ANIr-30—animals treated with anisomycin 30 min before irradiation; ANIr180—animals treated with anisomycin 180 min after irradiation; ANIr360—animals treated with anisomycin 360 min after irradiation. Scale bar is 40 μm; graphs right of the rows

only with anisomycin (AN group), as well as those treated with anisomycin 180 min or 360 min after irradiation (ANIr180 and ANIr360, respectively), was 100% (n = 4/4, per each group). The survival of animals treated with anisomycin 30 min before irradiation (ANIr-30 group) was 75% (n = 3/4). Fig. 2 demonstrates the effectivness of anisomycin as a radioprotector. The log-rank test indicated that the survival curves were significantly different between the Irr group and the CTRL and AN groups ($P < 0.05$), as well as between the Irr group and the groups of animals treated with anisomycin after irradiation (ANIr180 and ANIr360 groups; $P < 0.05$).

Immunohistochemistry of glial cells in the brain

To follow gliosis as the hallmark of neuroinflammation, we examined changes in glial activity in the somatosensory cortex, corpus callosum and brainstem. Coronal brain tissue sections were immunohistochemically stained for microglia (Iba-1) and astroglia (GFAP). Immunohistochemistry revealed the presence of a significantly decreased Iba-1 staining in all three studied brain structures (somatosensory cortex, corpus callosum, brainstem), in all three treatment groups, ANIr-30, ANIr180 and ANIr360 (panel rows in Fig. 3b, d and f), as compared to the Irr group (panel rows in Fig. 3a, c and e; one-way ANOVA for repeated measures with Dunnett's post hoc test gave treatment mean square (MS) = 4.916, $F = 5.344$ and $P = 0.026$). In other words, anisomycin significantly reduced Iba-1 marker expression irrespective of the brain region and time of administration with radiation (Fig. 3g, i and k). We also noted morphological changes of microglial cells between groups in the cerebral somatosensory cortex (panel rows in Fig. 3a and b). Namely, in the Irr group (Fig. 3, panel in row a), as compared to the naïve CTRL (Fig. 3, panel in row a), microglial cells had larger somata, whereas in the radioprotected groups, ANIr-30, ANIr180 and ANIr360 (Fig. 3, panels in row b), they had smaller somata size and rarely exhibited cell processes. Interestingly, astrogliosis was not apparent following irradiation in any of the studied brain structures, except for a trend for increased GFAP expression compared to the CTRL group (shown in Fig. 3h, j and l). Likewise, neither anisomycin treatment induced significant change in the GFAP staining compared to the Irr group.

Raman spectra analysis of brain areas

Raman spectra were recorded in coronal sections from the somatosensory cortex, corpus callosum and the brainstem. The average and normalized Raman spectra with the most significant bands from the corpus callosum and brainstem tissue are shown in Fig. 4 (Raman spectrum of the somatosensory cortex was not significantly different from the one for the corpus callosum and thus is omitted from the figure).

The assignation of the observed bands was done according to Movasaghi *et al.* [17] and is shown in Table 1. We followed the changes in bands attributed to the amino acids tryptophan (758, 1360 and 1616 cm^{-1}), tyrosine (823, 850 cm^{-1}), phenylalanine (1003 cm^{-1}) and proline (925 cm^{-1}). Also, changes in bands for nucleic acids, DNA and RNA (667, 780, 959, 1373, 1515 cm^{-1}), as well as for cholesterol (702 cm^{-1}), carbohydrates (877 cm^{-1}), lipid compounds (1066, 1304, 1442 cm^{-1}), combining lipids and proteins bands (1128, 1270, 1657 cm^{-1}) and phospholipids and nucleic acids bands (1089 cm^{-1}) were examined. We noticed that bands attributed to lipids as well as the mutual bands for lipids and proteins were more pronounced in the corpus callosum in comparison to the brainstem (Fig. 4a and b), which could be explained by the different content of white and grey matter in these regions.

The difference spectra between the brainstems (Fig. 5a) from CTRL and Irr animals revealed a slight increase for phenylalanine (1003 cm^{-1}) due to irradiation, as well as a trend for a decrease in bands assigned to tryptophan at 1616 cm^{-1}, nucleic acids at 780, 959 and 1089 cm^{-1}, and the combined band of lipids and proteins at 1658 cm^{-1}. When compared with the Irr experimental group (difference spectra in Fig. 5b-d), animals treated with anisomycin at different time points showed a significant treatment effect related to a higher intensity of the band assigned to RNA (uracil ring mode) at 780 cm^{-1}. Two-way ANOVA, animals vs treatment, showed treatment $MS = 6.173$, $F = 59.182$ and $P < 0.001$ (post hoc Bonferroni test for multiple comparisons vs the Irr group gave for ANIr-30 $P < 0$ 0.001, for ANIr180 $P < 0.001$ and for ANIr360, $P < 0.05$; Fig. 5e), however this test also showed a significant interaction of both factors with $MS = 0.568$, $F = 5.449$ and $P < 0.001$. The band assigned to the PO_4^{3-} group from nucleic acids at 959 cm^{-1} was significantly higher in all radioprotected animals. Two-way ANOVA (animals vs treatment) showed treatment $MS = 0.118$, $F = 42.767$, $P < 0.001$ (post hoc Bonferroni test for multiple comparisons vs the Irr group gave for ANIr-30 $P < 0.001$, for ANIr180 $P < 0.001$ and for ANIr360 $P < 0.001$; Fig. 5f). Furthermore, the intensity of the band with a combined contribution of the C-C bond of the acyl backbone in lipids and phosphodiester groups of nucleic acids at 1089 cm^{-1} was also significantly higher in all three radioprotected experimental groups. Two-way ANOVA (animals vs treatment) showed treatment $MS = 0.035$, $F = 37.397$, $P < 0.001$ (post hoc Bonferroni test for multiple comparisons vs the Irr group gave for ANIr-30 $P < 0.001$, for ANIr180 $P < 0.05$ and for ANIr360 $P < 0.001$; Fig. 5g).

Raman spectra analysis also revealed changes in the intensity of bands of several amino acids—tryptophan, tyrosine, proline and phenylalanine, which were more intensive in groups with anisomycin application after irradiation. When compared to the Irr group of animals, significantly higher intensity of the band attributed to tyrosine (850 cm^{-1}) was seen and a significant treatment effect was confirmed for all experimental time points. Two-Way ANOVA, (animals vs treatment) showed treatment $MS = 0.778$, $F = 35.813$, $P < 0.001$ (post hoc Bonferroni test for multiple comparisons vs the Irr group gave for

Fig. 3. (continued) represent the average signal (pixel percentages) ± SEM in respective brain areas of each experimental group, for microglia, Iba-1 (green bars: (g)—somatosensory cortex, (i)—corpus callosum and (k)—brainstem) and for astrocytes, GFAP (red bars: (h)—somatosensory cortex, (j)—corpus callosum and (l)—brainstem). Three animals per experimental group were used (overall 48 data points per group for the somatosensory cortex, and 24 for corpus callosum and brainstem). $P < 0.05$ (One-way ANOVA with repeated measures, followed by Dunnett's post hoc test).

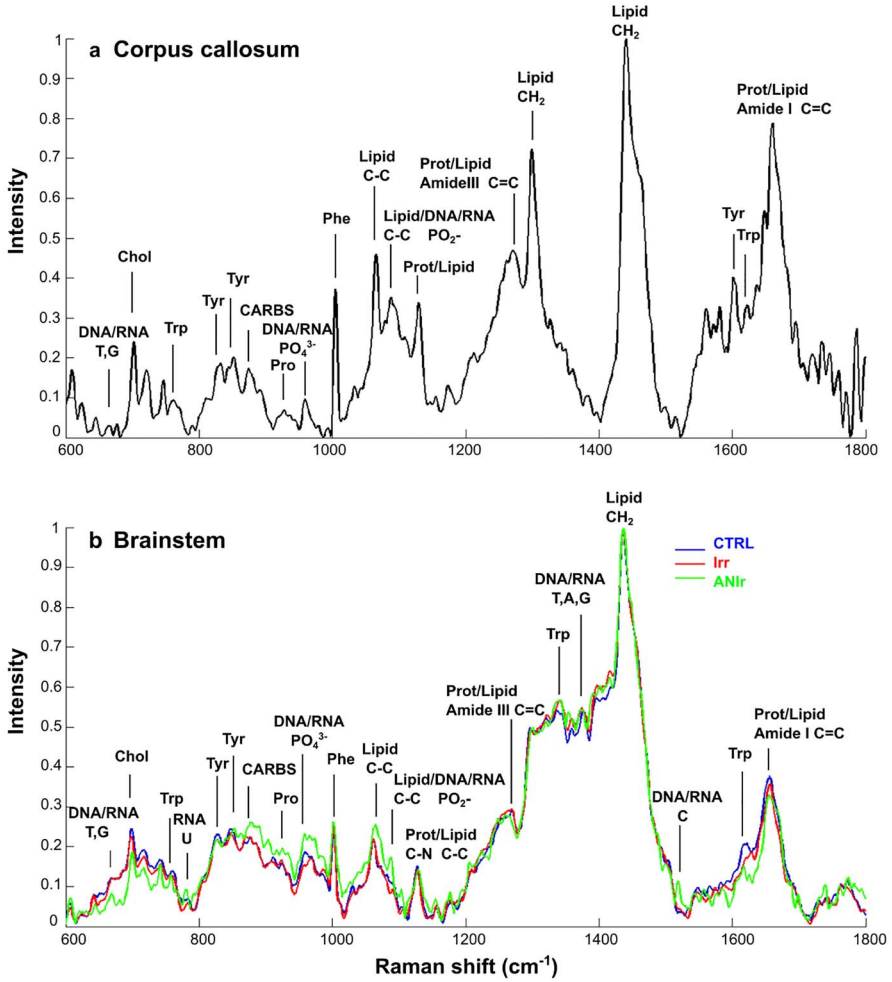

Fig. 4. Raman spectra of rat brain tissue. Average spectra of (a) control rat corpus callosum and (b) of brainstem control (CTRL), irradiated (Irr) and anisomycin-treated 30 min before radiation (ANIr). Cholesterol (Chol; 702 cm^{-1}), Tryptophan (Trp; 758, 1360, 1616 cm^{-1}), Tyrosine (Tyr; 823, 850 cm^{-1}), Carbohydrates (CARBS; 877 cm^{-1}), Proline (Pro; 925 cm^{-1}), Deoxyribonucleic acid/Ribonucleic acid (DNA/RNA): Thymine, Guanine (T, G; 667 cm^{-1}), Uracil (780 cm^{-1}), PO_4^{3-} (959 cm^{-1}), Adenine (T, G, A; 1373 cm^{-1}), Cytosine (1515 cm^{-1}), Phenylalanine (Phe; 1003 cm^{-1}), skeletal C-C stretch of lipids (1066 cm^{-1}), CH_2 deformation band in lipid (1304, 1442 cm^{-1}), C-C of acyl back-bone in lipid and phosphodiester band in nucleic acid (1089 cm^{-1}), C-N stretching of proteins & C-C of acyl backbone in lipid (1128 cm^{-1}), Amide III band in proteins (C-N stretch from α-helix) & C=C groups in unsaturated fatty acids and phospholipids (1270 cm^{-1}), Amide I band of proteins and C=C group in lipids (1657 cm^{-1}).

ANIr-30 $P = 0.85$, for ANIr180 $P < 0.001$ and for ANIr360 $P < 0.001$; Fig. 5h).

Effect of gamma rays and anisomycin treatment on IL-6, TNF-α and IL −10 content in blood plasma

To estimate the level of general inflammation (related to neuroinflammation), ELISA tests for two pro-inflammatory cytokines, IL-6 and TNF-α and the anti-inflammatory cytokine IL-10, were performed on blood plasma. Cytokine levels in the blood plasma of gamma irradiated, anisomycin treated and radioprotected animals were measured on the first, seventh and 28th day after treatment (Table 2; $P < 0.05$).

Already on the first day after treatment, irradiation induced a rise in the level of IL-6 compared to the CTRL group, but a significant difference was seen only on the seventh day. Also, as expected from previous work, there were no significant differences in TNF-α and IL-10 levels when compared with the CTRL group, although some rising trend in the former was seen on the first and 28th day after treatment [18].

Interestingly, in comparison with CTRL, the AN group caused a general increase of tested plasma cytokines at almost all treatment times. However, significant changes were observed for TNF-α on the first and 28th day, while a substantial increase of IL-6 was detected

Table 1. List of vibration bands in Raman spectra of brainstem tissue in the interval 600–1800 cm^{-1}. Assignation was done according to Movasaghi *et al.* [17]

Raman shift (cm^{-1})	Assignation
667	Thymine, Guanine
702	Cholesterol/sphingomyelin
758	Tryptophan
786	Uracil
823	Tyrosine
850	Tyrosine
877	Carbohydrates (CARBS)
925	Proline
959	PO_4^{3-}
1003	Phenylalanine
1066	Lipid, C-C stretch of lipid
1088	C-C skeletal band in lipid & phosphodiester band in nucleic acid
1128	C-N stretching of protein & C-C skeletal band in lipid
1270	Amide III band in protein & C=C groups in unsaturated fatty acid and phospholipid
1304	CH_2 deformation band in lipid
1360	Tryptophan
1373	Adenine, Guanine, Thymine
1442	CH_2 deformation band in lipid
1515	Cytosine
1616	Tryptophan
1657	Amide I band of proteins and C=C group in lipid

on the seventh day, remaining through the 28th day. In addition, a significant increase in the anti-inflammatory cytokine IL-10 was detected on the final 28th day.

Although anisomycin itself increased the plasma level of IL-6, we did not notice any changes on the first or seventh day if it was applied 30 minutes before irradiation (ANIr-30). Moreover, at these time points, the plasma level of IL-6 was almost the same as in the CTRL group, which, on the other hand, was at a lower level than in the Irr group, albeit without statistical significance. Surprisingly, with this treatment, the follow-up on the 28th day of plasma IL-6 cytokine showed a rising trend compared to the Irr group. This treatment also did not cause significant changes in the other two measured cytokines, pro-inflammatory TNF-α and anti-inflammatory IL-10, although we noted some rising trends.

Treatment with anisomycin 3 hours after irradiation (ANIr180) did not induce a significant change in the plasma levels of IL-6 and TNF-α compared to the Irr group. We noticed an increasing trend in plasma IL-6 level at later time points, the seventh and 28th day compared to Irr, indicating that the effect of anisomycin is more pronounced at later time points. The level of anti-inflammatory IL-10 also was increased at these two later time points compared to Irr, albeit only significantly on the 28th day.

Treatment with anisomycin 6 hours after irradiation (ANIr360) was generally more efficient in raising the level of cytokines than treatment at the other times. The anti-inflammatory cytokine IL-10 was significantly increased on the seventh day compared to the Irr group.

DISCUSSION

In this study, we tested the cellular and molecular mechanisms of anisomycin radioprotection in gamma-irradiated two-month-old male Wistar rats with the radioprotector applied at different times before or after radiation exposure.

Microglial cells, the resident innate immune cells in the brain, can be activated on exposure to specific agents, such as radiation, bacteria, or oxidative stress, leading to their release of pro-inflammatory cytokines and reactive oxygen species [19–22]. Our immunohistochemistry showed that anisomycin administered either before or after irradiation induces a decrease in Iba-1 staining of microglial cells in all three investigated brain areas (somatosensory cortex, corpus callosum and brainstem). This could be considered as a positive, inhibitory effect of anisomycin on cellular neuroinflammation. However, regarding the effect of radiation on cell shape we have noticed apparent changes only in microglia of the somatosensory cortex. The latter could be a consequence of lower dosage and radiation protocol, but also may be caused by the differences in the phenotypes of microglia in different parts of the brain, leading to region-specific responses of these cells to irradiation [23]. In fact, it was previously shown that irradiation activates microglia after single doses of >10 Gy and that lower doses lead to severe structural changes and cognitive impairment only months to years after irradiation [24–26].

Astrocytes are the most numerous glial cells in the CNS, playing an important role in the regulation of homeostasis, nutrient excretion and the metabolism of amino-acid based neurotransmitters [27, 28]. They have been shown to protect neurons and endothelial cells from

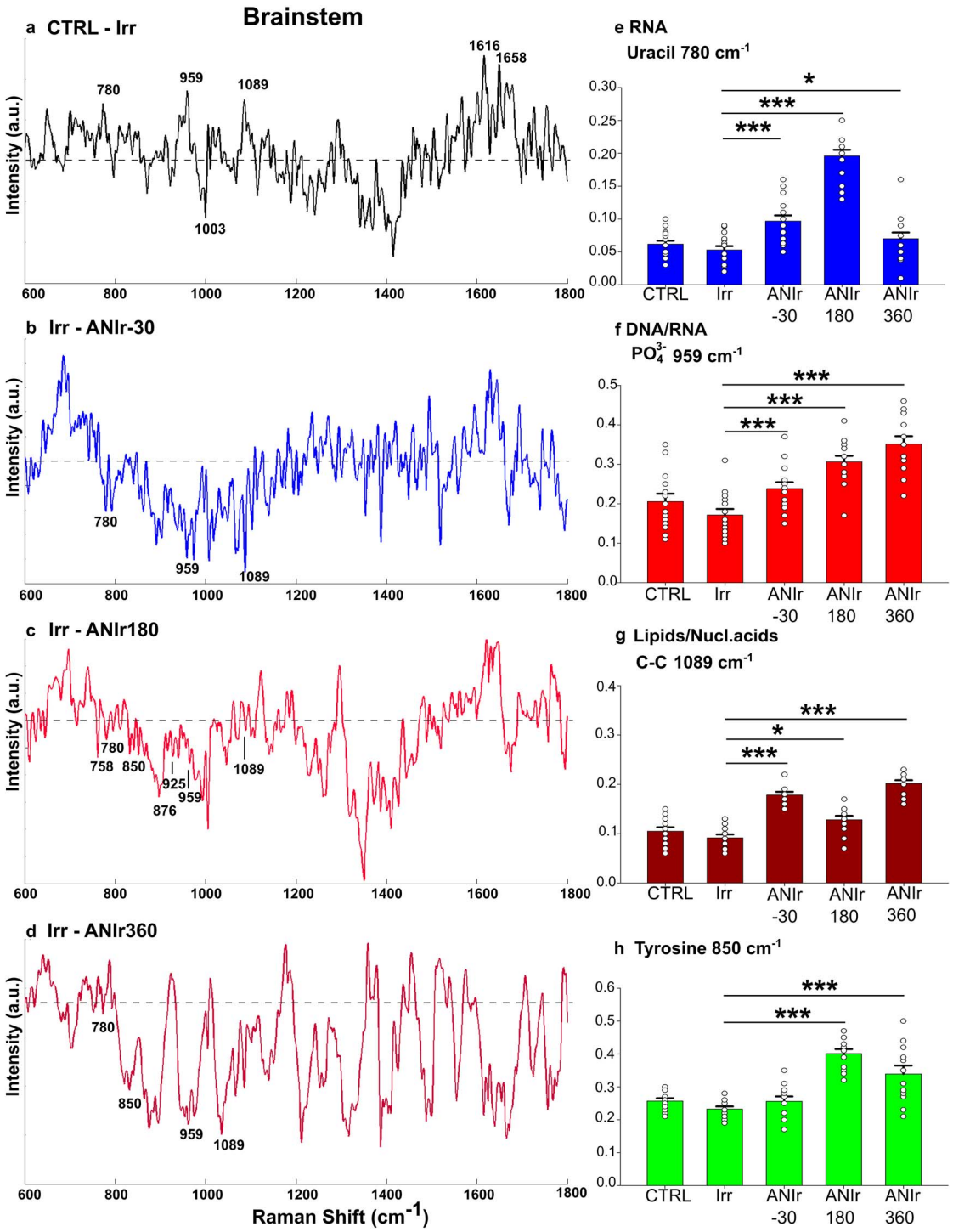

Fig. 5. Comparison of rat brainstem spectra after different treatments. Difference spectra between (a) control and irradiated rat brainstem tissue, (b) irradiated tissue and irradiated animals treated before radiation with anisomycin, (c) irradiated tissue and irradiated animals treated with anisomycin 3 h after radiation, (d) irradiated tissue and irradiated animals treated with anisomycin 6 h after radiation. Tryptophan (758, 1616 cm^{-1}), Deoxyribonucleic acid/Ribonucleic acid (DNA/RNA) - Uracil (780 cm^{-1}) & PO_4^{3-} (959 cm^{-1}), C-C skeletal of acyl back-bone in lipid and phosphodiester band in nucleic acids (1089 cm^{-1}), Phenylalanine (1003 cm^{-1}), Tyrosine (850 cm^{-1}), Proline (925 cm^{-1}). Ordinate: upward direction—lower value than in control or irradiated tissue; downward—higher than in control or irradiated tissue; (e)–(h) the intensities of bands with significances assigned to (e) Uracil (780 cm^{-1}), (f) PO_4^{3-} (959 cm^{-1}), (g) C-C (1089 cm^{-1}) and (h) Tyrosine (850 cm^{-1}). Three animals per experimental group were used. Data are presented as mean ± (SEM). Statistical analysis was performed using Two-way ANOVA with post hoc Bonferroni test. $^{*}P < 0.05$, $^{***}P < 0.001$.

Table 2. Effect of gamma irradiation and treatment with anisomycin on plasma cytokine levels

Groups	IL-6 (pg/ml)			TNF-α (pg/ml)			IL-10 (pg/ml)		
	Days after treatment			Days after treatment			Days after treatment		
	1	7	28	1	7	28	1	7	28
CTRL	294 ± 77	286 ± 57	399 ± 29	107 ± 23	162 ± 63	94 ± 29	224 ± 26	171 ± 25	214 ± 35
Irr	390 ± 56	527 ± 66*	307 ± 63	165 ± 37	178 ± 29	181 ± 39	169 ± 24	130 ± 23	183 ± 34
AN	729 ± 125	757 ± 211*	910 ± 61*	230 ± 13*	319 ± 62	326 ± 35*	183 ± 71	312 ± 65	375 ± 31*
ANIr-30	299 ± 156	285 ± 61	469 ± 101	242 ± 89	145 ± 39	233 ± 65	155 ± 36	197 ± 10	268 ± 30
ANIr180	375 ± 52	662 ± 144	493 ± 120	181 ± 30	275 ± 49	197 ± 59	191 ± 11	264 ± 63	305 ± 13#
ANIr360	578 ± 96	479 ± 90	635 ± 132	317 ± 39*	245 ± 96	337 ± 36*	230 ± 61	256 ± 6#	355 ± 70

Data presented as mean (± SEM) from rats/control or treated group. IL-6 = interleukin 6; TNF-α = tumor necrosis factor α: IL-10 = interleukin 10. CTRL = control intact animals (n = 4); Irr = irradiated animals (n = 3); AN = animals only treated with antibiotic anisomycin (n = 4); ANIr-30 = animals treated with anisomycin 30 minutes before irradiation (n = 3); ANIr180 = animals treated 180 minutes after irradiation (n = 4); ANIr360 = animals treated 360 minutes after irradiation (n = 4). Statistical analysis was performed using one way ANOVA with Holm-Sidak method post hoc test. Significant changes with treatments are presented in comparison to the CTRL group (*) or to the Irr group (#), and $P < 0.05$ were considered as statistically significant.

oxidative stress [29, 30]. In our experiments, the observed increase in GFAP in all three studied brain structures of irradiated animals was not significant. This again could be due to a lower dose of applied radiation and the whole body irradiation protocol. Likewise, no anisomycin treatment affected astrocytes GFAP staining significantly, although an interesting trend of decreased GFAP staining was observed when anisomycin was applied alone.

Of note, anisomycin alone caused no significant changes in the markers or the morphology of microglia and astrocytes, suggesting that anisomycin itself has no impact on these cell types.

Several studies have shown that anisomycin induces an increase in amino acids such as tryptophan, tyrosine, phenylalanine and proline in the murine brain [31,32]. We confirm this finding here with Raman microspectroscopy when anisomycin is applied after irradiation. We also noticed increased intensities of tentative spectral markers of radioprotection related to the PO_4^{3-} band of nucleic acids, the C-C bond of the acyl backbone in lipids and the phosphodiester groups of nucleic acids, as well as the band related to RNA (uracil ring mode) at 780 cm^{-1}. In accordance with these data, Koshiba *et al.* reported that anisomycin may induce and stabilize mRNAs [33]. Stabilization of RNA could thus be a mechanism by which anisomycin exerts its radioprotective activity in the brain.

Humoral factors of inflammation (that are related to neuroinflammation) were also followed. Upon tissue irradiation, pro-inflammatory cytokines can be rapidly activated, acting in synergy with ionizing radiation by generating free radical species. On the other hand, anti-inflammatory cytokines act in parallel to restore homeostasis [34]. The brain and the immune system are in bidirectional communication [35]. However, it cannot be ruled out that changes in circulating cytokines observed here may also reflect inflammation in radiosensitive tissues other than the brain. The fact that anisomycin activates p38 kinases, which in turn regulate TNF-α production, is underscored by the effect of anisomycin alone, which gives an apparent increase in TNF-α from day one [7, 36]. MAPKs such as p38 are important intracellular mediators of signal transduction that react in response to a wide variety of stimuli and agents such as hypoxia, osmotic stress, oxidation, antibiotics and radiation. The suggested neuroprotective role of p38 MAPK could be of importance because MAPK pathways regulate TNF-α production by both transcriptional and post-transcriptional mechanisms [8, 37]. Consequently, the production of TNF-α is tightly regulated to prevent exaggerated or persistent inflammation [38, 39]. In our experiments with anisomycin alone, an increase in TNF-α is followed by an increase in IL-6, which is known to be produced in response to the former pro-inflammatory cytokine [40]. In addition, IL-6 is known to induce the expression of multiple factors with anti-inflammatory properties, one of them being IL-10 [41]. Indeed, we found here for anisomycin application to naïve animals that at later time points IL-10 does show a rise. It was demonstrated that IL-6 acts in concert with IL-10 at the translational level, inhibiting TNF-α protein expression by astrocytes [42]. Nevertheless, as reported here, TNF-α is still abundant on day 28, but we can also note a tandem action of IL-6 and IL-10 occurring at the end of the experimental course opposing the TNF-α rise. Thus, our results support the idea that anisomycin reduced neuroinflammation, as suggested by a decrease in Iba-1 staining together with cytokine changes, consistent with an increased anti-inflammatory response. Nevertheless, the changes in the pro-inflammatory cytokines are complex and require further investigation.

It should be noted that the effect of anisomycin as a radioprotector became apparent only at later times of application. Particularly, at 6 h after irradiation (ANIr360) we recorded a rise in TNF-α which was in fact significant on the first and last day of the experiment. The same mechanism can apply to the ANIr180 group as well, where also a fine-tuning between the pro- and anti-inflammatory cytokines occurs. It can thus be proposed that anisomycin as the putative p38 activator is not necessarily detrimental to the brain. In fact, the survival in both ANIr180 and ANIr360 groups was 100%. Interestingly though, anisomycin applied before radiation (ANIr-30) gave a relatively lower survival of 75% (3/4) while no significant changes in cytokine levels occurred. A hypothesis may be proposed that radiation interacts with the action of the radioprotector. To check this hypothesis, additional studies on a larger numbers of animals are needed.

In conclusion, our study demonstrates that anisomycin can overcome effects of gamma radiation, particularly at later times of application (thus identifying it as a radioprotector of utility in radiation accidents). Being a translational inhibitor and a true MAPK signaling agonist, this radioprotector may act as a primary or secondary stimulus for humoral and cellular immune responses.

ACKNOWLEDGEMENTS

We would like to thank our veterinarians, Miloš Jovanović, Miloš Ćućko and Miodrag Milovanović, for assisting in animal care and handling. The authors thank Dr. Boris Šakić, for the help in data statistics. We are grateful to Dr. Joel C. Glover for expert help in text editing. The authors are also thankful to the Faculty of Medicine, Institute of Anatomy, University of Belgrade for enabling access to the tissue processing equipment.

FUNDING

This work was supported by the Ministry of education, science and technological development of the Republic of Serbia, contract number: 451-03-68/2020-14/200178.

CONFLICT OF INTEREST

The authors declare that they have no conflict of interests.

ETHICS

Permission from the Ethical commission of the Faculty of Biology, University of Belgrade (approval number EK-BF-2016/08).

REFERENCES

1. Balentova S, Adamkov M. Molecular, cellular and functional effects of radiation-induced brain injury: a review. *Int J Mol Sci* 2015;16:27796–815.
2. Gu J, Zhu S, Li X et al. Effect of Amifostine in head and neck cancer patients treated with radiotherapy: a systematic review and meta-analysis based on randomized controlled trials. *PLoS One* 2014;9:e95968.
3. Nieder C, Andratschke NH, Wiedenmann N, Molls M. Prevention of radiation-induced central nervous system toxicity: a role for Amifostine? *Anticancer Res* 2004;24:3803–9.
4. Jovanovic M, Šećerov B, Bačić G. The potential of in vivo EPR in evaluating free radical reactions in irradiated rats and mechanisms of radioprotection. In: Čupić Ž, Anić S (eds). *Physical Chemistry 2016 (Proceedings)*. Belgrade: Society of Physical Chemists, 2016, 491–4.
5. Grollman AP. Inhibitors of Protein Biosynthesis: II. Mode of action of anisomycin. *J Biol Chem* 1967;242:3226–33.
6. Barbacid M, Vazquez D. [3H]anisomycin binding to eukaryotic ribosomes. *J Mol Biol* 1974;84:603–23.
7. Hazzalin CA, le Panse R, Cano E, Mahadevan LC. Anisomycin selectively desensitizes signalling components involved in stress kinase activation and Fos Andjun Induction. *Mol Cell Biol* 1998;18:1844–54.
8. Zheng S, Zuo Z. Isoflurane preconditioning induces neuroprotection against ischemia via activation of P38 mitogen-activated protein kinases. *Mol Pharmacol* 2004;65:1172–80.
9. Hong S-S, Qian H, Zhao P et al. Anisomycin protects cortical neurons from prolonged hypoxia with differential regulation of p38 and ERK. *Brain Res* 2007;1149:76–86.
10. Kharlamov E, Cagnoli CM, Atabay C et al. Opposite effect of protein synthesis inhibitors on potassium deficiency-induced apoptotic cell death in immature and mature neuronal cultures. *J Neurochem* 2002;65:1395–8.
11. Cohen H, Kaplan Z, Matar MA et al. Anisomycin, a protein synthesis inhibitor, disrupts traumatic memory consolidation and attenuates posttraumatic stress response in rats. *Biol Psychiatry* 2006;60:767–76.
12. Tolić L, Grujić S, Mojović M et al. Determination of anisomycin in tissues and serum by LC-MS/MS: application to pharmacokinetic and distribution studies in rats. *RSC Adv* 2016;6:92479–89.
13. Scoccianti S, Detti B, Gadda D et al. Organs at risk in the brain and their dose-constraints in adults and in children: a radiation oncologist's guide for delineation in everyday practice. *Radiother Oncol* 2015;114:230–8.
14. Lawrence YR, Li XA, Naqa I et al. Radiation dose–volume effects in the brain. *Int J Radiat Oncol Biol Phys* 2010;76:S20–7.
15. Wanisch K, Wotjak CT. Time course and efficiency of protein synthesis inhibition following intracerebral and systemic anisomycin treatment. *Neurobiol Learn Mem* 2008;90:485–94.
16. Swanson LW. *Brain Maps: Structure of the Rat Brain*, 2nd edn. Amsterdam: Elsevier Science, 1998, 45–191.
17. Movasaghi Z, Rehman S, ur Rehman DI. Fourier Transform Infrared (FTIR) Spectroscopy of Biological Tissues. *Appl Spectrosc Rev* 2008;43:134–79.
18. Kočović DM, Bajuk-Bogdanović D, Maslovarić I et al. Raman spectral analysis of the brainstem and responses of neuroglia and cytokines in whole-body gamma-irradiated rats after administration of aminothiol-based radioprotector GL2011. *Arch Biol Sci* 2021; in press.
19. Babior BM. Phagocytes and oxidative stress. *Am J Med* 2000;109:33–44.
20. Block ML, Zecca L, Hong J-S. Microglia-mediated neurotoxicity: uncovering the molecular mechanisms. *Nat Rev Neurosci* 2007;8:57–69.
21. Lee WH, Sonntag WE, Mitschelen M et al. Irradiation induces regionally specific alterations in pro-inflammatory environments in rat brain. *Int J Radiat Biol* 2010;86:132–44.
22. Conner KR, Forbes ME, Lee WH et al. AT1 receptor antagonism does not influence early radiation-induced changes in microglial activation or neurogenesis in the normal rat brain. *Radiat Res* 2011;176:71–83.
23. Xuan F-L, Chithanathan K, Lilleväli K et al. Differences of microglia in the brain and the spinal cord. *Front Cell Neurosci* 2019;13:504.
24. Tofilon PJ, Fike JR. The radio response of the central nervous system: a dynamic process. *Radiat Res* 2000;153:357–70.

25. Greene-Schloesser D, Robbins ME, Peiffer AM et al. Radiation-induced brain injury: a review. *Front Oncol* 2012; 2:73.
26. Ramanan S, Kooshki M, Zhao W et al. PPARα ligands inhibit radiation-induced microglial inflammatory responses by negatively regulating NF-κB and AP-1 pathways. *Free Radic Biol Med* 2008;45:1695–704.
27. Allaman I, Bélanger M, Magistretti PJ. Astrocyte–neuron metabolic relationships: for better and for worse. *Trends Neurosci* 2011;34:76–87.
28. Schousboe A, Scafidi S, Bak LK et al. Glutamate metabolism in the brain focusing on astrocytes. In: Parpura V, Schousboe A, Verkhratsky A (eds). *Glutamate and ATP at the Interface of Metabolism and Signaling in the Brain*, Vol. 11. Cham: Springer International Publishing, 2014, 13–30.
29. Wilson JX. Antioxidant defense of the brain: a role for astrocytes. *Can J Physiol Pharmacol* 1997;75:1149–63.
30. Bylicky MA, Mueller GP, Day RM. Mechanisms of endogenous neuroprotective effects of astrocytes in brain injury. *Oxid Med Cell Longev* 2018;2018:6501031.
31. Rainbow TC, Hoffman PL, Flexner LB. Studies of memory: a reevaluation in mice of the effects of inhibitors on the rate of synthesis of cerebral proteins as related to amnesia. *Pharmacol Biochem Behav* 1980;12:79–84.
32. Schweri MM, Carr LA. Effects of amino acid alterations caused by protein synthesis inhibitors on brain monoamine formation. *Neuropharmacology* 1982;21:839–45.
33. Koshiba T, Ballas N, Wong L-M et al. Transcriptional regulation of PS-IAA4/5andPS-IAA6 early gene expression by indoleacetic acid and protein synthesis inhibitors in pea (Pisum sativum). *J Mol Biol* 1995;253:396–413.
34. Schaue D, Kachikwu EL, McBride WH. Cytokines in radiobiological responses: a review. *Radiat Res* 2012;178:505–23.
35. Dantzer R. Neuroimmune interactions: from the brain to the immune system and vice versa. *Physiol Rev* 2018;98:477–504.
36. Cano E, Doza Y, Ben-Levy R et al. Identification of anisomycin-activated kinases p45 and p55 in murine cells as MAPKAP kinase-2. *Oncogene* 1996;12:805–12.
37. Sabio G, Davis RJ. TNF and MAP kinase signalling pathways. *Semin Immunol* 2014;26:237–45.
38. Rutault K, Hazzalin CA, Mahadevan LC. Combinations of ERK and p38 MAPK inhibitors ablate tumor necrosis factor-α (TNF-α) mRNA induction. Evidence for selective destabilization of TNF-alpha transcripts. *J Biol Chem* 2001;276:6666–74.
39. Deleault KM, Skinner SJ, Brooks SA. Tristetraprolin regulates TNF TNF-α mRNA stability via a proteasome dependent mechanism involving the combined action of the ERK and p38 pathways. *Mol Immunol* 2008;45:13–24.
40. Cesaris PD, Starace D, Riccioli A et al. Tumor necrosis factor-α induces interleukin-6 production and integrin ligand expression by distinct transduction pathways. *J Biol Chem* 1998;273:7566–71.
41. Ahmed ST, Ivashkiv LB. Inhibition of IL-6 and IL-10 signaling and stat activation by inflammatory and stress pathways. *J Immunol* 2000;165:5227–37.
42. Benveniste EN, Tang LP, Law RM. Differential regulation of astrocyte TNF-alpha expression by the cytokines TGF-beta, IL-6 and IL-10. *Int J Dev Neurosci* 1995;13:341–9.